Ying Fan,[1,2] Xuezhu Li,[1] Wenzhen Xiao,[1] Jia Fu,[1] Ray C. Harris,[3] Maja Lindenmeyer,[4] Clemens D. Cohen,[4] Nicolas Guillot,[1] Margaret H. Baron,[5] Niansong Wang,[2] Kyung Lee,[1] John C. He,[1,6] Detlef Schlondorff,[1] and Peter Y. Chuang[1]

BAMBI Elimination Enhances Alternative TGF-β Signaling and Glomerular Dysfunction in Diabetic Mice

BMP, activin, membrane-bound inhibitor (BAMBI) acts as a pseudo-receptor for the transforming growth factor (TGF)-β type I receptor family and a negative modulator of TGF-β kinase signaling, and BAMBI$^{-/-}$ mice show mild endothelial dysfunction. Because diabetic glomerular disease is associated with TGF-β overexpression and microvascular alterations, we examined the effect of diabetes on glomerular BAMBI mRNA levels. In isolated glomeruli from biopsies of patients with diabetic nephropathy and in glomeruli from mice with type 2 diabetes, BAMBI was downregulated. We then examined the effects of BAMBI deletion on streptozotocin-induced diabetic glomerulopathy in mice. BAMBI$^{-/-}$ mice developed more albuminuria, with a widening of foot processes, than BAMBI$^{+/+}$ mice, along with increased activation of alternative TGF-β pathways such as extracellular signal–related kinase (ERK)1/2 and Smad1/5 in glomeruli and cortices of BAMBI$^{-/-}$ mice. *Vegfr2* and *Angpt1*, genes controlling glomerular endothelial stability, were downmodulated in glomeruli from BAMBI$^{-/-}$ mice with diabetes. Incubation of glomeruli from nondiabetic BAMBI$^{+/+}$ or BAMBI$^{-/-}$ mice with TGF-β resulted in the downregulation of *Vegfr2* and *Angpt1*, effects that were more pronounced in BAMBI$^{-/-}$ mice and were prevented by a MEK inhibitor. The downregulation of Vegfr2 in diabetes was localized to glomerular endothelial cells using a histone yellow reporter under the Vegfr2 promoter. Thus, BAMBI modulates the effects of diabetes on glomerular permselectivity in association with altered ERK1/2 and Smad1/5 signaling. Future therapeutic interventions with inhibitors of alternative TGF-β signaling may therefore be of interest in diabetic nephropathy.

Diabetic nephropathy (DN) is the leading cause of chronic kidney disease and end-stage kidney failure in the western world. In DN, early glomerular changes are characterized by mesangial cell hypertrophy with mesangial matrix expansion and thickening of the glomerular basement membrane (GBM) (1), which is followed by broadening and effacement of the podocyte foot process (FP) with proteinuria and eventually a reduction in podocyte density (2). Increased activity of transforming growth factor (TGF)-β may contribute to these changes (3,4) because inhibition of TGF-β mitigates mesangial matrix overexpression, renal hypertrophy, and podocyte loss, with eventual glomerulosclerosis, in rodent models of DN (5–7). The signaling pathways involved have been attributed mostly to canonical TGF-β signaling, which involves ligand binding of TGF-β to its cognate receptors (i.e., ALK5/type I and type II TGF-β receptors), followed by activation of Smad2 and 3 transcription factors (8). Surprisingly, while interfering with Smad-3 signaling in experimental diabetic animal studies markedly diminished glomerular matrix changes, it had minimal effects on preventing the development of proteinuria in experimental models of DN (9,10). This invites the speculation that alternative TGF-β signaling, such as Smad1 and -5 (11) and extracellular signal–related kinase (ERK)1/2 (12–15),

---

[1]Department of Medicine, Division of Nephrology, Icahn School of Medicine at Mount Sinai, New York, NY
[2]Department of Nephrology, Shanghai Jiao Tong University Affiliated Sixth People's Hospital, Shanghai, China
[3]Vanderbilt University School of Medicine, Nashville, TN
[4]Division of Nephrology and Institute of Physiology with Center of Integrative Human Physiology, University Hospital and University of Zurich, Zurich, Switzerland
[5]Tisch Cancer Institute and Department of Medicine, Division of Hematology and Medical Oncology, Icahn School of Medicine at Mount Sinai, New York, NY
[6]Renal Section, James J. Peter Veterans Administration Medical Center, Bronx, NY

might contribute to glomerular changes and thereby to the proteinuria of DN.

Longstanding diabetes also causes macro- and microvascular complications. Indeed, global endothelial dysfunction is closely associated with diabetes (16); in particular, abnormal glomerular angiogenesis has been described in individuals with DN (17). Thus, the endothelium, and especially the glomerular endothelium, may be a prominent target for damage in longstanding diabetes (16), which has been linked to the development of proteinuria as a hallmark of DN (18,19). Furthermore, gene expression analysis of experimental DN, as well as biopsies of patients with DN, show prominent changes in endothelial gene expression consistent with glomerular endothelial cell dysfunction (20,21).

In contrast to its effect on epithelial cells and fibroblasts, the action of TGF-β on endothelial cells is mediated predominantly by the ALK1 rather than the ALK5 TGF-β type 1 receptor, resulting in alternative TGF-β signaling (22–25), with activation of Smad1/5 and ERK1/2 pathways and neoangiogenesis (26–29). We demonstrated previously that genetic deletion of BMP, activin, membrane bound inhibitor (BAMBI) alters in vitro and in vivo angiogenesis (30,31). BAMBI functions as a dominant negative, nonsignaling, pseudo-receptor for members of the TGF-β type I receptor family to negatively modulates TGF-β signaling (32–34). In human umbilical vein endothelial cells, BAMBI predominantly influences the response to TGF-β via ALK1-mediated phosphorylation of SMAD1/5 and ERK1/2 to promote angiogenesis in vitro (30). Mice with genetic elimination of BAMBI (BAMBI$^{-/-}$) develop exaggerated compensatory renal glomerular endothelial hypertrophy after unilateral nephrectomy (30) and accelerated re-endothelialization and neovascularization after arterial injury (31). Consistent with our observations, ERK1/2 activation contributed to vascular remodeling in different model systems (27–29).

Because glomerular endothelial dysfunction is a prominent feature of DN and BAMBI$^{-/-}$ mice display accentuated endothelial response after endothelial injury, herein we examined whether BAMBI plays a pathogenic role in the development of diabetic glomerular injury.

RESEARCH DESIGN AND METHODS

Animal Models

BAMBI$^{-/-}$ mice on a C57BL/6 background were generated as reported elsewhere (35). *Flk1*:H2B-EYFP mice were described previously (36). Diabetes was induced in 6- to 8-week-old BAMBI$^{+/+}$ and BAMBI$^{-/-}$ mice by five consecutive daily intraperitoneal injections of low-dose streptozotocin (STZ) (50 mg/kg). Littermate BAMBI$^{+/+}$ and BAMBI$^{-/-}$ mice injected with a citrate buffer served as controls. Urine and blood samples were collected at indicated time points, and all mice were killed 18 weeks after the initial STZ injection. All animal studies were performed in accordance with the guidelines of and were approved by the Institutional Animal Care and Use Committee at the Icahn School of Medicine at Mount Sinai, New York, NY.

Noninvasive Blood Pressure Measurement By Tail Cuff Manometry

Blood pressure was measured using the CODA noninvasive tail cuff blood pressure system (Kent Scientific, Torrington, CT) (37). Mice were acclimated to the tail cuff manometer and restraining device five times per week for 2–3 weeks before the day of actual data acquisition.

Urine/Serum Analyses

Urine albumin was quantified using an ELISA kit (Bethyl Laboratory, Houston, TX), and urine creatinine was quantified using a QuantiChrom Creatinine Assay Kit (DICT-500; Bioassay Systems). Serum creatinine was measured using a high-performance liquid chromatography–based method following a previously published protocol (38).

Tissue Histology and Morphometry

Kidney sections were fixed and embedded in paraffin, as previously described (39,40). For transmission electron microscopy, kidney cortex samples fixed in 2.5% glutaraldehyde were sectioned and mounted on a copper grid; then images were photographed using a Hitachi H7650 microscope (Tokyo, Japan), as previously described (40). Morphometric analysis and quantification of mesangial expansion, FP width, and GBM thickness was carried out using ImageJ software (National Institutes of Health, Bethesda, MD) on digitized transmission electron microscopy images, as previously described (39,40).

Western Blot Analysis

Glomerular isolation, lysate preparation, and Western blotting were performed as previously described (41). Each lane contained 30 to 60 μg of total protein. Semiquantitative assessment of band density was performed using ImageJ software (National Institutes of Health). Band density for the protein of interest was normalized to either GAPDH or β-actin. Antibodies against phospho- and total Erk1/2, as well as phospho- and total Smad proteins, were purchased through Cell Signaling Technology (Danvers, MA). β-Actin antibody was purchased from Sigma-Aldrich (St. Louis, MO).

Quantitative Real-Time PCR

Real-time PCR was performed as previously described (39–41). Cycle threshold (Ct) values of the gene targets were normalized to GAPDH. Fold change in expression of target genes compared with the reference group was calculated using the $2^{-\Delta\Delta CT}$ method, with GAPDH as the calibrator. Sequences of primers used are supplied in the Supplementary Table 2.

Immunofluorescence Staining

Staining, image acquisition, and fluorescence intensity quantification were performed as previously described

(39,40). The rabbit antibody to WT-1 was from Novus Biologicals (Littleton, CO), the rat antibody to CD31, from R&D Systems (Minneapolis, MN), the mouse monoclonal antibody to synaptopodin, from Fitzgerald Industries International (Acton, MA), and the rabbit antibody to vimentin, from Cell Signaling (Danvers, MA).

Glomerular Isolation and Incubation

Mouse glomeruli were isolated as previously described (42) and transferred onto a 6-cm tissue culture dish coated with type I collagen and with RPMI 1640 medium supplemented with 10% FBS and 1% penicillin/streptomycin. Glomeruli were allowed to attach overnight at 37°C in an incubator, and they were serum starved for 6–8 h in RPMI medium before being stimulated with TGF-β (1 ng/mL) for 6 h. Where specified, 2 μmol/L of MAPK/ERK kinase (MEK) inhibitor U1026 (Calbiochem) was added to the culture medium 30 min before the addition of TGF-β.

Quantitative Real-Time PCR of Human Renal Biopsies

Human renal biopsy specimens were collected in an international multicenter study, the European Renal cDNA Bank-Kröner-Fresenius biopsy bank (ERCB-KFB) (43). Diagnostic renal biopsies were obtained from patients after informed consent and with approval of local ethics committees. Following renal biopsy, the tissue was immediately transferred to an RNase inhibitor and microdissected into glomerular and tubular fragments (43). Total RNA was isolated from microdissected glomeruli and was reversely transcribed according to a protocol previously reported (43). Predeveloped TaqMan reagents were used for human BAMBI (NM_012342.2), as well as the reference gene, 18S rRNA (Applied Biosystems). The expression of the candidate gene was normalized to 18S rRNA. mRNA expression was analyzed using standard curve quantification.

Statistical Analysis

Data are expressed as mean $\pm$ SEM. Statistical analyses were performed using GraphPad Prism software. For comparison of means between groups, one- or two-way ANOVA was performed, followed by the Bonferroni post-test. Results were considered significant if $P < 0.05$.

RESULTS

Glomerular BAMBI Expression Is Suppressed in Human and Murine Models of DN

To delineate the pathogenic role of BAMBI in diabetic glomerular injury, we first investigated the glomerular expression of BAMBI in human and murine models of DN. Using quantitative RT-PCR determinations, we compared the glomerular expression of BAMBI in kidney biopsies of healthy living donors (LDs) who received a kidney transplant with that in patients with established DN, arterionephrosclerosis, or focal segmental glomerulosclerosis. The salient clinical patient data are presented in Supplementary Table 1. Glomerular BAMBI mRNA transcript levels in DN were approximately two-thirds of the values of those of LDs (0.65 ± 0.28 vs. 1.00 ± 0.10; $P = 0.036$) (Fig. 1A). A similar degree of reduction in glomerular BAMBI mRNA expression also was observed in focal segmental glomerulosclerosis biopsies (0.70 ± 0.08; $P = 0.020$), but not in arterionephrosclerosis biopsies (1.19 ± 0.17; $P = 0.23$), when both were compared with LD biopsies. Glomerular expression of BAMBI was similarly reduced in a robust murine model of type 2 diabetes with accelerated DN: *db/db; eNOS$^{-/-}$* mice on a C57BL/6 background (44) (Fig. 1B).

Physiologic and Biochemical Parameters of Diabetic BAMBI$^{-/-}$ Mice

Since glomerular BAMBI expression is suppressed in diabetic kidney disease and BAMBI$^{-/-}$ mice exhibit accentuated alternative TGF-β signaling and altered endothelial response after injury (30,31,45), we examined the pathogenic role of BAMBI deficiency in DN by comparing
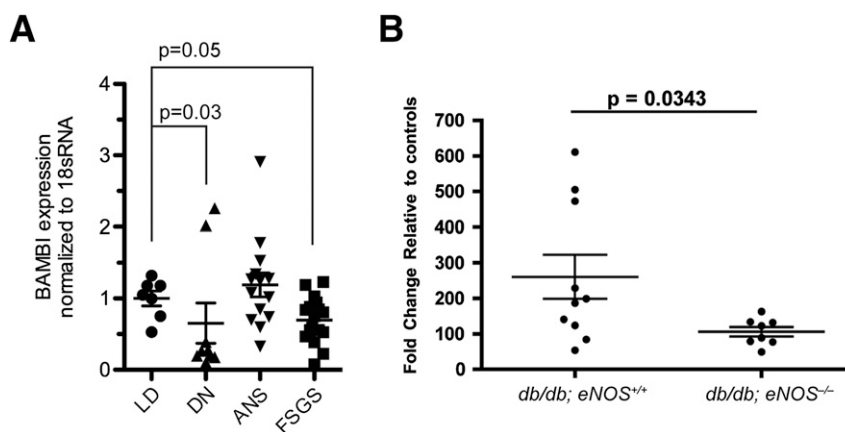

Figure 1—*A*: Levels of mRNA for BAMBI normalized to 18S RNA were determined by quantitative RT-PCR in glomeruli isolated from kidney biopsies of healthy LD transplants (*n* = 7) and of patients with established DN (*n* = 11), arterionephrosclerosis (ANS; *n* = 14), or focal segmental glomerulosclerosis (FSGS; *n* = 17). *P* values refer to group comparisons with LD values using the Kruskal-Wallis and a subsequent Mann-Whitney *U* test. *B*: Relative changes in mRNA levels for BAMBI determined in glomeruli isolated from *db/db;eNOS*$^{+/+}$ (*n* = 10) or *db/db;eNOS*$^{-/-}$ (*n* = 8) mice as a model of type 2 diabetes with accelerated DN. *P* value refers to group comparison by unpaired *t* test.

the development of diabetic glomerular injury in BAMBI$^{-/-}$ and BAMBI$^{+/+}$ mice with STZ-induced diabetes. We used fully back-crossed mice on a C57BL/6 background, which develop only a mild phenotype (46), because we expected to see more pronounced changes in the BAMBI$^{-/-}$ mice because of their enhanced TGF-β signaling (30,32,33). Age-matched BAMBI$^{+/+}$ and BAMBI$^{-/-}$ littermate mice were used; the BAMBI$^{-/-}$ mice had a slightly lower body weight at the time of DM induction, as previously observed (45) (Table 1). Both BAMBI$^{+/+}$ and BAMBI$^{-/-}$ mice developed comparable degrees of hyperglycemia after STZ injection over the 18-week study (Fig. 2A). Consistent with polyuria induced by hyperglycemia, both diabetic BAMBI$^{+/+}$ and BAMBI$^{-/-}$ mice gained significantly less weight compared with control nondiabetic (i.e., citrate-injected) BAMBI$^{+/+}$ and BAMBI$^{-/-}$ mice (Fig. 2B). Systolic and diastolic blood pressures in trained mice, determined using tail cuff methodology (37), and serum creatinine concentrations measured by high-performance liquid chromatography were also not significantly different between the two diabetic groups (Table 1). Overall kidney weight–to–body weight ratios were not different between the groups and increased by 44% in BAMBI$^{-/-}$ and by 36% in BAMBI$^{+/+}$ mice, consistent with diabetic renal hypertrophy. As expected for C57BL/6 mice, urinary albumin excretion, determined either as timed urine collection (albumin per 24 h; Table 1) or as a random urine albumin-to-creatinine ratio, was modestly elevated among diabetic BAMBI$^{+/+}$ mice compared with nondiabetic BAMBI$^{+/+}$ mice (Fig. 2C). Notably, urinary albumin excretion in diabetic BAMBI$^{-/-}$ mice was more than double that of diabetic BAMBI$^{+/+}$ mice (Fig. 2C and Table 1), indicating that BAMBI deficiency exacerbates proteinuria as a marker of diabetic glomerular injury.

Glomerular Morphometric Characteristics of Diabetic BAMBI$^{-/-}$ Mice

All diabetic mice developed significant mesangial expansion at 18 weeks compared with their corresponding nondiabetic controls (Fig. 3A and B); the expansion in BAMBI$^{-/-}$ and BAMBI$^{+/+}$ mice was comparable. Based on ultrastructural comparisons, the width of podocyte FPs revealed significantly wider FPs in diabetic BAMBI$^{-/-}$

mice compared with diabetic BAMBI$^{+/+}$ mice (Fig. 3C and D). The thickness of GBMs increased significantly in all diabetic mice, but they were not different between diabetic BAMBI$^{+/+}$ and diabetic BAMBI$^{-/-}$ mice (Fig. 3E). No consistent glomerular endothelial morphological abnormalities were detected by light or electron microscopy in either group. There were also no abnormalities noted in the tubulointerstitial compartment, consistent with early and a mild degree of diabetic glomerulopathy.

ERK1/2 and Smad1/5 Phosphorylation Is Enhanced in Glomeruli or Cortices of Diabetic BAMBI$^{-/-}$ Mice Compared With Diabetic BAMBI$^{+/+}$ Mice

Activation of glomerular ERK1/2 and Smad-2/3 has been noted in diabetic mice and rats (4,14,15,47). We therefore compared the phosphorylation of ERK1/2, Smad1/5, and Smad3 in isolated glomeruli and cortices obtained from BAMBI$^{+/+}$ and BAMBI$^{-/-}$ mice with or without diabetes for 18 weeks. Among nondiabetic, citrate-injected mice, phosphorylation of ERK1/2 in glomeruli (Fig. 4A) or cortices (Supplementary Fig. 1) of BAMBI$^{-/-}$ mice was not different from that of BAMBI$^{+/+}$ mice (Fig. 4A). ERK1/2 phosphorylation increased in glomeruli and cortices of the diabetic mice, but it was higher in BAMBI$^{-/-}$ than BAMBI$^{+/+}$ mice (Fig. 4A and Supplementary Fig. 1). Because results from isolated glomeruli (from two different mice per experimental group) and cortices (from three different mice per experimental group) were comparable, these were combined for statistical evaluation by densitometry (Fig. 4B).

Phosphorylation of Smad1/5 was already higher in glomeruli of nondiabetic, citrate-injected BAMBI$^{-/-}$ mice than in BAMBI$^{+/+}$ mice, and it increased further only in glomeruli of diabetic BAMBI$^{-/-}$ mice (Fig. 4C and D). By contrast, activation of the canonical TGF-β signaling pathway (as assessed by phosphorylation of Smad3) was higher in glomeruli of both groups of diabetic mice compared with the respective nondiabetic, citrate-injected controls, and this was enhanced in diabetic BAMBI$^{-/-}$ compared with diabetic BAMBI$^{+/+}$ mice (Fig. 4E and F).

Consistent with the phosphorylation/activation data for ERK1/2, the expression of respective target genes for

Table 1—Physiological and biochemical parameters

Parameters	BAMBI$^{+/+}$ citrate ($n = 6$)	BAMBI$^{-/-}$ citrate ($n = 5$)	BAMBI$^{+/+}$ STZ ($n = 7$)	BAMBI$^{-/-}$ STZ ($n = 8$)
	Groups			
Body weight before injection (g)	23.57 ± 1.7	19.6 ± 0.6	24.1 ± 1.8	21.80 ± 1.4
Kidney–to–body weight ratio (mg/g)	7.2 ± 0.4	6.7 ± 0.4	9.9 ± 0.6*Δξ	9.6 ± 0.5*Δ
Blood pressure (mmHg)				
Systolic	98 ± 5	105 ± 3	110 ± 6	100 ± 8
Diastolic	77 ± 6	79 ± 3	80 ± 6	70 ± 7
Serum creatinine (mg/dL)	0.16 ± 0.02	0.16 ± 0.01	0.17 ± 0.01	0.14 ± 0.004
Urinary albumin excretion (μg/24 hours)	21.9 ± 3.9	31.5 ± 8.7	103.8 ± 11 *Δ	207.0 ± 32 *Δξ

*$P < 0.05$ vs. BAMBI$^{+/+}$ citrate. Δ$P < 0.05$ vs. BAMBI$^{-/-}$ citrate. ξ$P < 0.05$ vs. BAMBI$^{+/+}$ STZ.
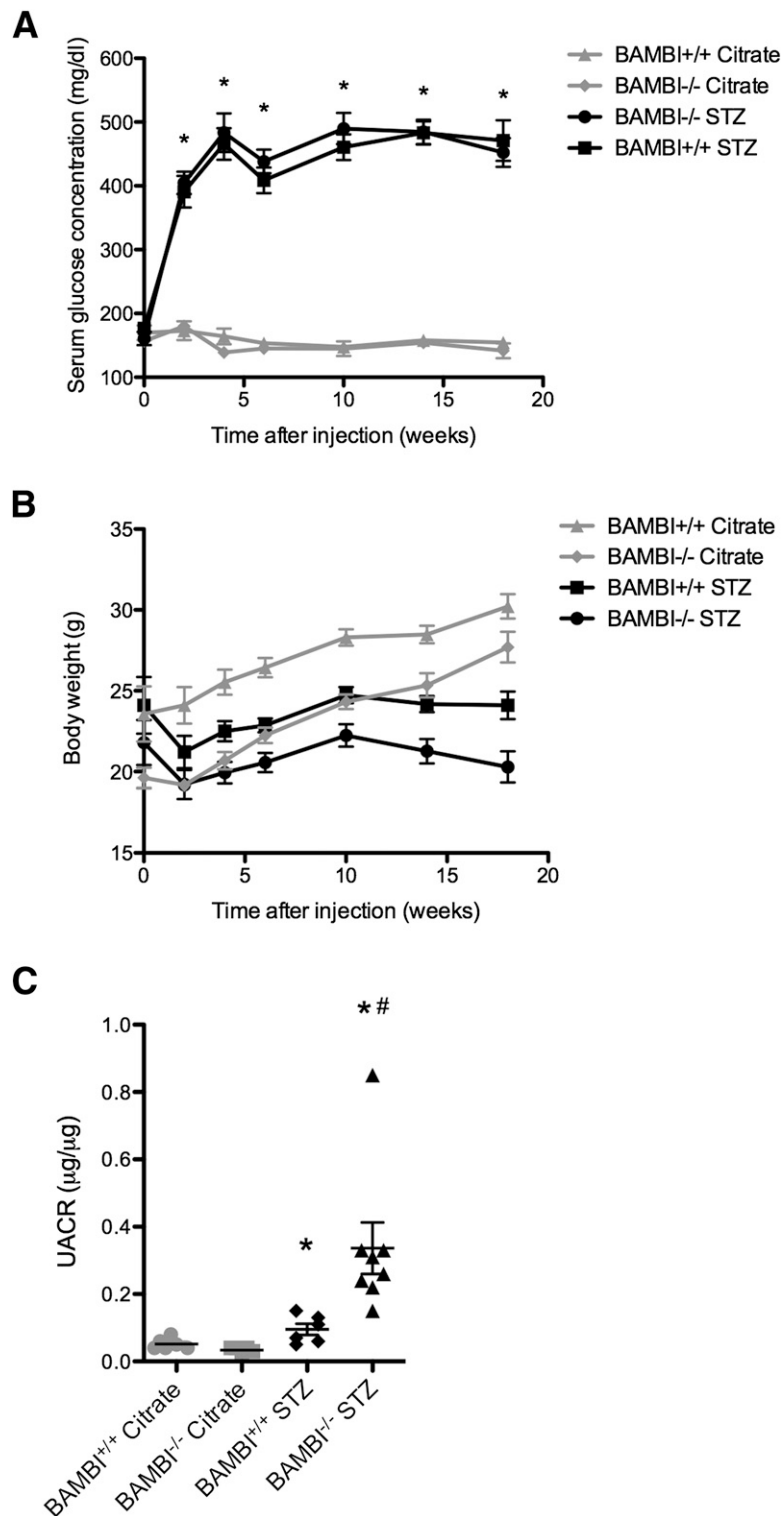
Figure 2—*A*: Age-matched BAMBI$^{+/+}$ and BAMBI$^{-/-}$ mice were injected with STZ as described in RESEARCH DESIGN AND METHODS. Both groups developed comparable degrees of hyperglycemia when compared with citrate-injected controls during the 18-week study period (n = 5 for BAMBI$^{+/+}$ citrate-injected mice; n = 7 for BAMBI$^{-/-}$ citrate-injected mice; n = 7 for BAMBI$^{+/+}$ STZ-induced diabetic mice; and n = 8 for BAMBI$^{-/-}$ STZ-induced diabetic mice). *P < 0.05 compared with citrate-injected controls. *B*: BAMBI$^{-/-}$ mice tended to weigh less than BAMBI$^{+/+}$ littermates at the time of citrate or STZ injection, and both diabetic BAMBI$^{+/+}$ and BAMBI$^{-/-}$ mice gained significantly less weight compared with nondiabetic (e.g., citrate-injected) BAMBI$^{+/+}$ and BAMBI$^{-/-}$ control mice during the 18-week study period. *C*: After 18 weeks of diabetes, the urinary albumin-to-creatinine ratio (UACR) of diabetic BAMBI$^{+/+}$ mice was significantly, but only modestly, elevated compared with that of nondiabetic BAMBI$^{+/+}$ mice; it was, however, more than twice as elevated in diabetic BAMBI$^{-/-}$ mice. *P < 0.05 compared with the respective citrate-injected controls; #P < 0.05 compared with the respective BAMBI$^{+/+}$ STZ-injected mice.
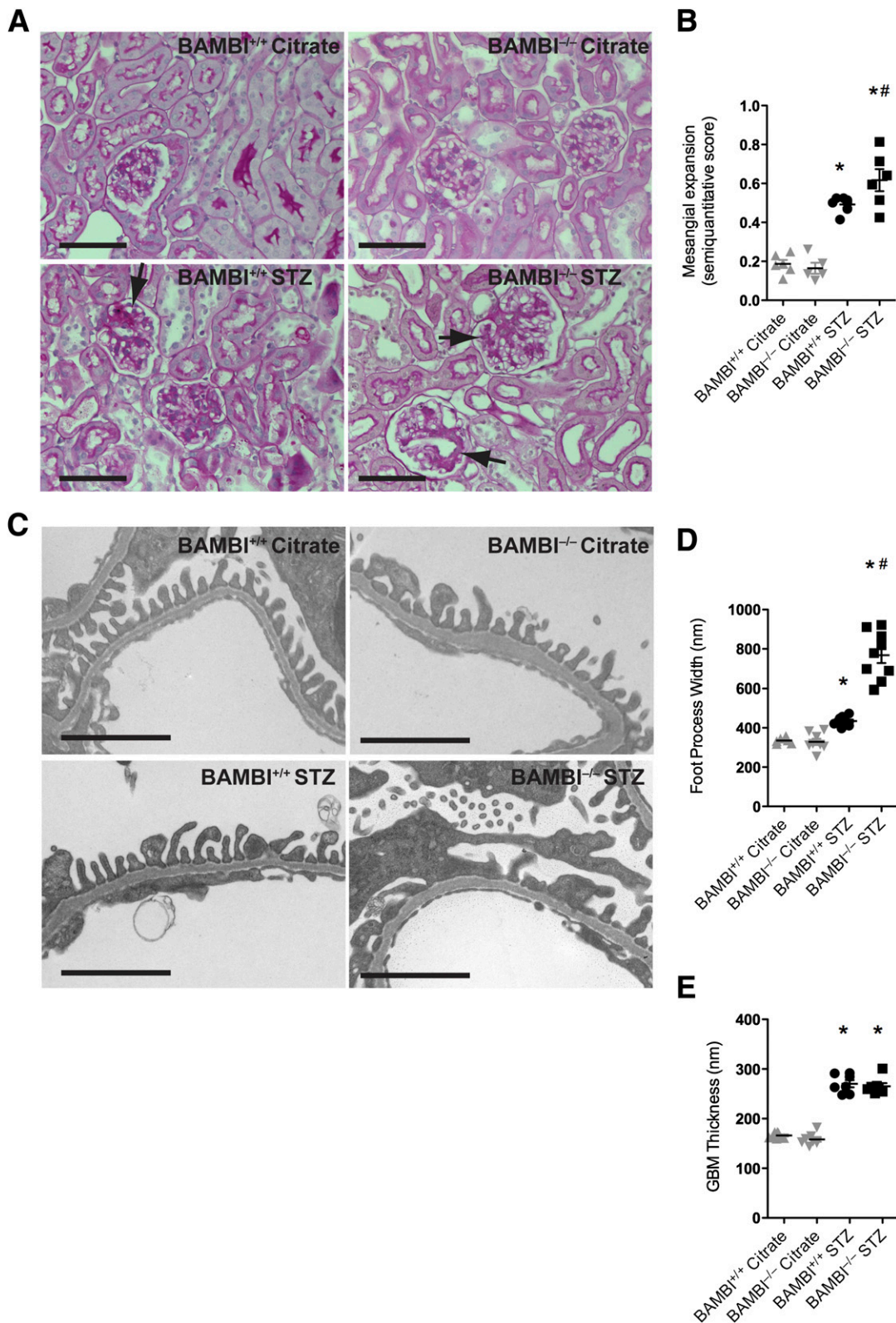
Figure 3—*A*: Light microscopy images (hematoxylin and eosin stains) from renal cortices of BAMBI$^{+/+}$ and BAMBI$^{-/-}$ mice 18 weeks after either citrate or STZ injection showing mesangial accentuation in the diabetic mice. Bars indicate 50 µm. *B*: Semiquantitative evaluation of the mesangial expansion determined in five mice per group, with an average of 30 glomeruli evaluated for each mouse. *C*: Representative electron microscopy images from glomeruli of the four groups after 18 weeks of the study. Bars indicate 2 µm. *D* and *E*: Quantification shows significantly broader FPs in the glomeruli of diabetic BAMBI$^{-/-}$ mice compared with BAMBI$^{+/+}$ mice but a comparable increase in GBM thickening in both strains of diabetic mice. Results are from measurements performed in two or three glomeruli from three mice per group. *$P < 0.05$ compared with the respective citrate-injected controls; #$P < 0.05$ compared with the respective BAMBI$^{+/+}$ STZ-injected mice.
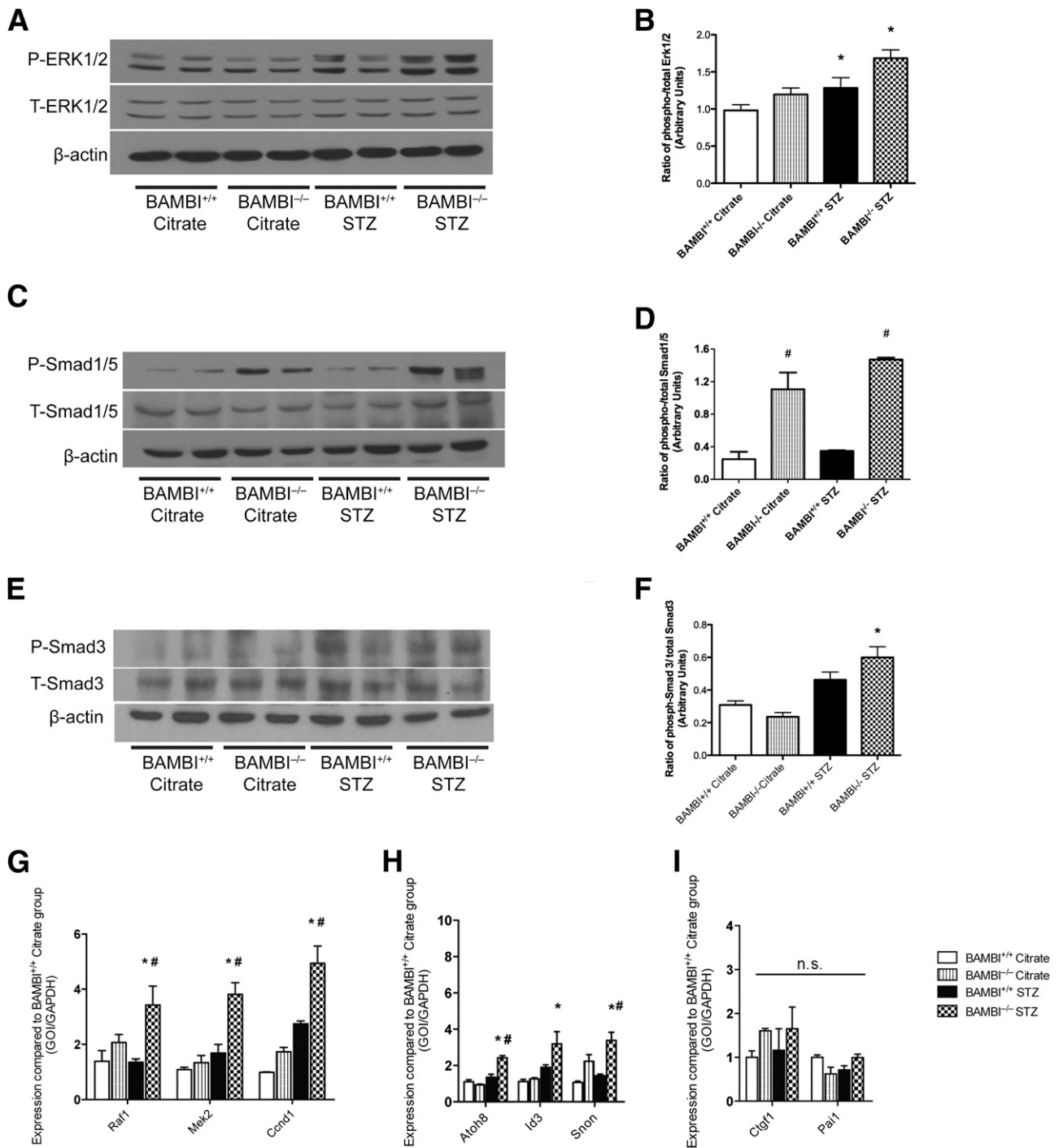
Figure 4—ERK1/2 and Smad phosphorylation in glomeruli isolated from BAMBI$^{+/+}$ and BAMBI$^{-/-}$ mice 18 weeks after citrate or STZ injection. *A*, *C*, and *E*: Glomerular extracts were prepared and probed on Western blots with antibodies directed against the phosphorylated (P) or unphosphorylated total (T) form of ERK1/2, Smad1/5, and Smad3, as described in RESEARCH DESIGN AND METHODS. β-Actin served as the loading control. Results shown are from two representative mice per group. *B*: Combined results obtained for ERK1/2 phosphorylation by densitometric evaluation of the Western blots form two different but comparable experimental series: one using extracts of isolated glomeruli from two mice per group and one using cortical extracts from three mice per group (Supplementary Fig. 1). Group statistics were performed on the five samples per group. Densitometry results for the phosphorylation of Smad1/5 (*D*) and Smad3 (*E*) are shown. Levels of mRNA of respective target genes for ERK1/2 (*Raf1*, *Mel2*, *Ccnd1*) (*G*) and for Smad1/5 (*Atoh8*, *Id3*, and *Snon*) (*H*) were significantly higher in the glomeruli isolated from diabetic BAMBI$^{-/-}$ mice compared with those from diabetic BAMBI$^{+/+}$ mice. *I*: Smad2/3 target genes *Ctgf1* and *Pai1* were not different between the diabetic BAMBI$^{-/-}$ mice and diabetic BAMBI$^{+/+}$ mice. *$P < 0.05$ compared with the respective citrate-injected controls; #$P < 0.05$ compared with the respective BAMBI$^{+/+}$ STZ-injected mice. GOI, gene of interest; n.s., not significant.

ERK1/2 (48), such as *Raf1*, *Mel2*, and *Ccnd1*, and for Smad1/5 (49), such as *Atoh8*, *Id3*, and *Snon*, was significantly higher in the glomeruli of diabetic BAMBI$^{-/-}$ mice compared with diabetic BAMBI$^{+/+}$ mice (Fig. 4*G*). By contrast, Smad3 target genes *Ctgf1* and *Pai1* were not different between the diabetic BAMBI$^{-/-}$ mice and the diabetic BAMBI$^{+/+}$ mice (Fig. 4*H*). Taken together, these data indicate that signaling through ERK1/2 and Smad1/5 is enhanced in glomeruli from diabetic mice with deletion of BAMBI compared with wild-type diabetic mice, whereas Smad3 signaling in glomeruli is less affected by BAMBI deletion after 18 weeks of STZ-induced diabetes.

Glomerular Expression of Angiogenic Factors Is Altered in Diabetic BAMBI$^{-/-}$ Mice

We previously reported that BAMBI elimination influences the endothelial phenotype (30,31), and endothelial growth factors influence the microvascular disease of diabetes, including in glomeruli (50–55). We therefore examined the expression of endothelial growth factors and their receptors in glomeruli isolated from control and diabetic BAMBI$^{+/+}$ and BAMBI$^{-/-}$ mice. Levels of mRNA for Vegf-A, angiopoietin 2 (Angpt2), and Tie2 were comparable in glomeruli isolated from (STZ-induced) diabetic mice irrespective of their BAMBI genotype (data not shown). By contrast, expression of Vegfr2, but not Vegfr1, was significantly reduced in glomeruli of both citrate-injected and STZ-induced diabetic BAMBI$^{-/-}$ mice compared with diabetic or citrate-injected BAMBI$^{+/+}$ mice (Fig. 5*A*). Angpt1 mRNA levels were significantly reduced in glomeruli from BAMBI$^{-/-}$ mice with STZ-induced diabetes compared with either their citrate-injected controls or the diabetic BAMBI$^{+/+}$ mice (Fig. 5*A*). BAMBI mRNA levels were not reduced in the glomeruli of BAMBI$^{+/+}$ C57BL/6 mice after 18 weeks of diabetes with mild DN (Fig. 5*A*), which is in contrast to the results obtained in a model of severe DN in *db/db;eNOS*$^{-/-}$ mice (Fig. 1).

To determine whether the reduced levels of mRNA for Vegfr2 and Angpt1 in the glomeruli from diabetic BAMBI$^{-/-}$ mice resulted from enhanced TGF-β signaling, freshly isolated glomeruli from BAMBI$^{+/+}$ and BAMBI$^{-/-}$ control mice were incubated with TGF-β ex vivo, and mRNA levels for Vegfr1 and 2 and Angptn1 were determined. As shown in Fig. 5*B*, mRNA levels of Vegfr1 were comparable in glomeruli from either BAMBI$^{+/+}$ or BAMBI$^{-/-}$ mice and were not changed by TGF-β. By contrast, TGF-β reduced mRNA levels of Vegfr2 and Angpt1 in glomeruli from both BAMBI$^{+/+}$ and BAMBI$^{-/-}$ mice, but this effect was significantly greater in glomeruli from BAMBI$^{-/-}$ mice (Fig. 5*B*). To determine whether the increased downregulation of Vegfr2 expression by TGF-β in glomeruli of BAMBI$^{-/-}$ mice is mediated through enhanced alternative TGF-β signaling, glomeruli were incubated with or without the MEK antagonist U0126 to inhibit ERK1/2 activation (Fig. 5*C*). Again, TGF-β decreased the levels of Vegfr2 and Angpt1 mRNA in glomeruli from both BAMBI$^{+/+}$ and BABMI$^{-/-}$

mice, and these effects were abrogated by the inhibitor U0126 for ERK1/2 activation (Fig. 5*C*).

To evaluate further the expression of the *Vegfr2* gene in glomerular endothelial cells, we took advantage of a transgenic mouse (back-crossed into the C57BL/6 strain) expressing a histone H2B-yellow fluorescent protein (EYFP) fusion reporter under the control of Vegfr2/Flk1 regulatory sequences (Flk1:H2B-EYFP [36]). We first intercrossed the transgene into our BAMBI$^{+/+}$ and BAMBI$^{-/-}$ mice. As shown in Fig. 6*A*, in adult BAMBI$^{+/+}$ and BAMBI$^{-/-}$ mice, expression of histone yellow is restricted to the nuclei of some glomerular cells, which upon CD31 double stain were identified as endothelial cells (Supplementary Fig. 2). The restriction of the *Vegfr2* gene to the glomerulus in kidneys from adult mice is consistent with previous observations (36) and with the importance of persistent Vegfr2 expression in glomerular endothelial cells for their normal function (54,55). Colocalization with Hoechst stain confirmed the nuclear localization of the H2B-EYFP reporter and its restricted expression (representing endothelial cells) in about 30% of total glomerular cells (Fig. 6*A*). The numbers and fluorescence intensity of H2B-EYFP-positive endothelial cells per glomerular area were comparable between nondiabetic BAMBI$^{+/+}$ and BAMBI$^{-/-}$ mice (Fig. 6*B* and *C*). After 18 weeks of diabetes, the intensity of H2B-EYFP fluorescence was significantly reduced in glomeruli of BAMBI$^{-/-}$ but not BAMB$^{+/+}$ mice (Fig. 6*A* and *C*). In diabetic BAMBI$^{-/-}$ mice, a 50% loss of H2B-EYFP-positive nuclei was observed (Fig. 6*A* and *B*). This decrease was not caused by cell loss because the number of Hoechst-positive nuclei per glomerular area did not change. We also determined the glomerular endothelial area using CD31 as an endothelial marker and computer-assisted morphometry. As shown in Supplementary Fig. 3, CD31-positive areas per glomerulus in kidneys from BAMBI$^{-/-}$ than BAMBI$^{+/+}$ mice were not significantly different after 18 weeks of diabetes. Finally, we also excluded that changes in podocyte numbers (as determined by WT-1-positive nuclei per glomerulus) might contribute to the observed effects in BAMBI$^{-/-}$ mice with 18 weeks of diabetes compared with BAMBI$^{+/+}$ mice. As expected in mice with a C57BL/6 background, no change in podocyte numbers was noted (Supplementary Fig. 4). Taken together with the mRNA levels in glomeruli isolated from the diabetic mice, these data are consistent with significantly reduced expression of vascular endothelial growth factor (VEGF) receptor-2 in glomerular endothelial cells of diabetic BAMBI$^{-/-}$ mice compared with their citrate-injected controls or to diabetic BAMBI$^{+/+}$ mice.

DISCUSSION

Our results show that genetic elimination of BAMBI as a modulator of the signaling of the family of TGF cytokines renders the almost-resistant C57BL/6 mouse strain more susceptible to the development of diabetic glomerular abnormalities, as determined by proteinuria with a widening of the FPs. This is associated with
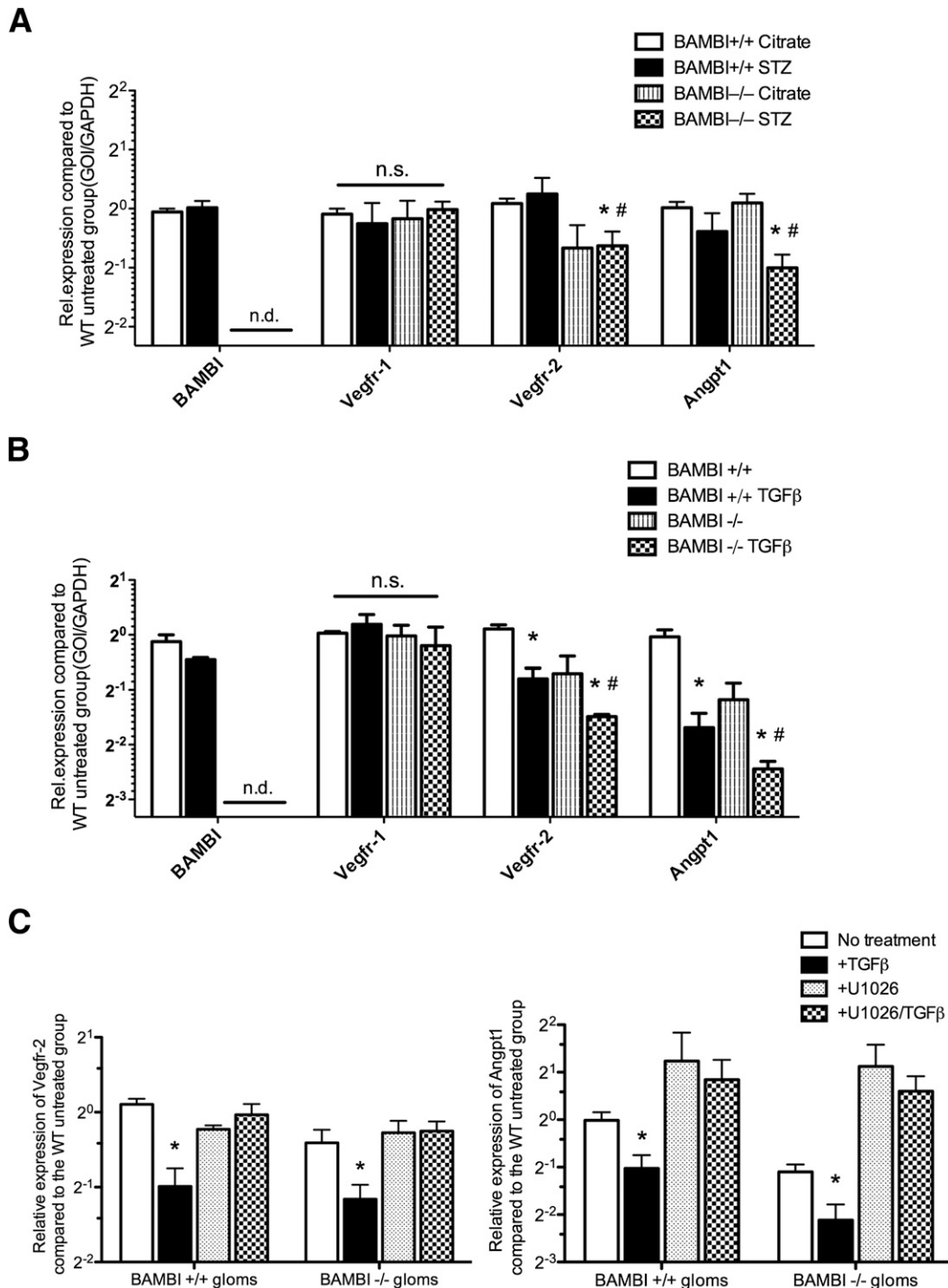
Figure 5—*A*: Levels of mRNA for angiogenic factors and their receptors in glomeruli isolated from BAMBI^{+/+} and BAMBI^{−/−} mice 18 weeks after either citrate or STZ injection. Results are means ± SEMs of triplicate determinations using glomeruli from three to six mice per group. *$P < 0.05$ compared with the respective citrate-injected controls; #$P < 0.05$ compared with the respective BAMBI^{+/+} STZ-injected mice. *B*: Levels of mRNA for angiogenic factors or their receptors obtained after incubation of isolated glomeruli from BAMBI^{+/+} or BAMBI^{−/−} mice under control conditions or with addition of TGF-β for 6 h before extraction and quantitative RT–PCR, as described in RESEARCH DESIGN AND METHODS. Results are means ± SEMs from three to five separate incubations and glomerular preparations per group. *$P < 0.05$ compared with the respective vehicle-treated glomeruli; #$P < 0.05$ compared with the TGF-β-treated BAMBI^{+/+} glomeruli. *C*: Levels of mRNA expression for Vegfr2 and Angpt1 in glomeruli (gloms) isolated from either BAMBI^{+/+} or BAMBI^{−/−} mice after incubation under either basal conditions or with TGF-β, U1026, or TGF-β plus U1026. Results are from three to six experiments per group. *$P < 0.05$ compared with U1026 or U1026/TGF-β-treated groups. GOI, gene of interest; n.s., not significant; n.d., not detectable; WT, wild type.
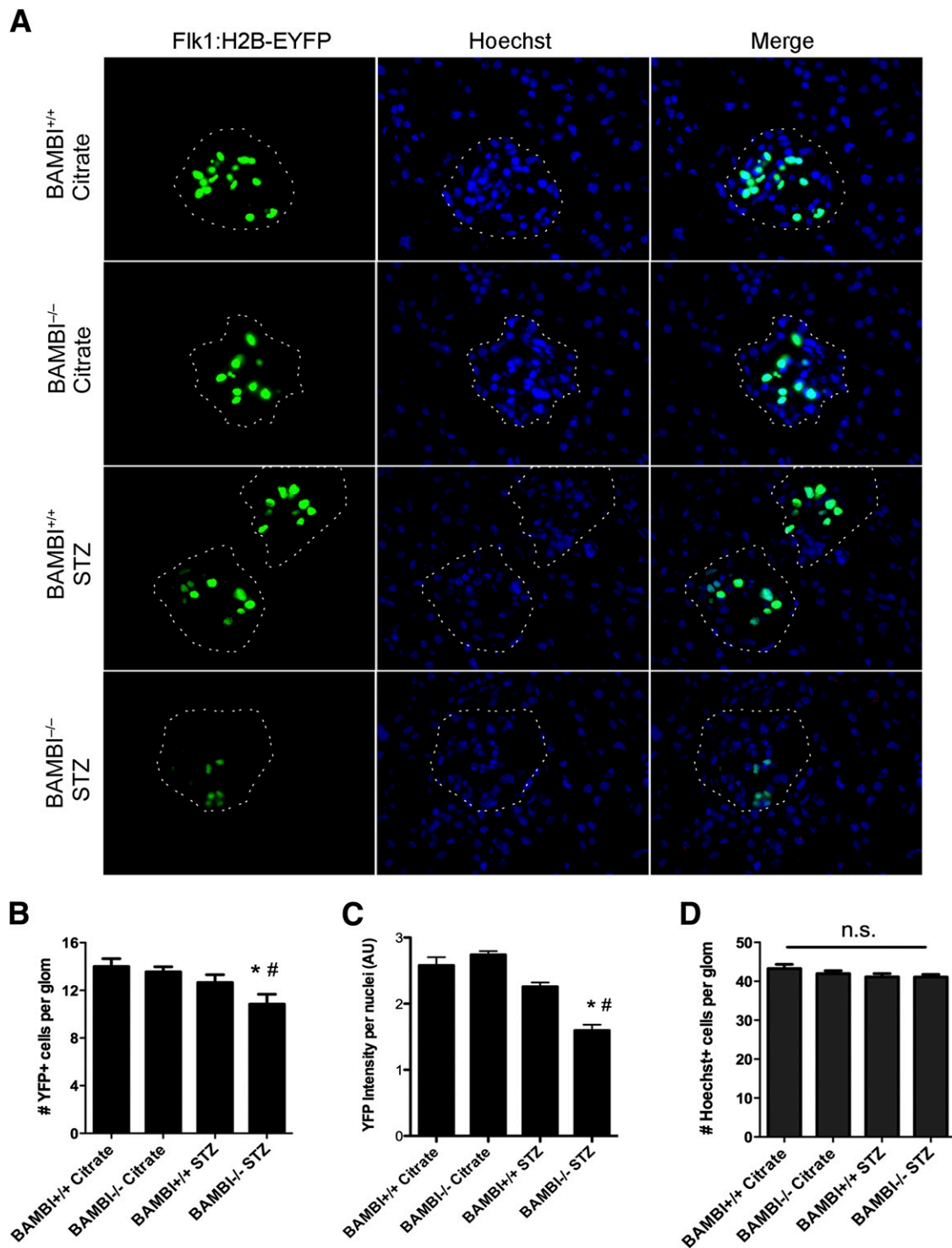
Figure 6—*A*: Immunofluorescence images from kidneys of BAMBI$^{+/+}$ or BAMBI$^{-/-}$ mice expressing the histone yellow fluorescent protein (H2B-EYFP) under the control of Vegfr-2/Flk1 regulatory sequences (Flk-1:H2B-EYFP transgene) and stained with Hoechst nuclear dye. Each fluorescence channel is shown individually and as a merged image. Images are from BAMBI$^{+/+}$ and BAMBI$^{-/-}$ mice 18 weeks after either citrate or STZ injection. The dotted lines outline the glomerular capsules as visualized by phase-contrast microscopy. *B–D*: Quantification of the number (*B*) and intensity of fluorescence for H2B-EYFP-positive cell nuclei representing endothelial cells (*C*), and the number of total glomerular cell nuclei (Hoechst stain) per glomerular outline. Results are means ± SEMs of four or five glomeruli evaluated per animal (two mice per group). *$P < 0.05$ compared with the respective citrate-injected controls; #$P < 0.05$ compared with BAMBI$^{+/+}$ STZ-injected mice. AU, arbitrary units; glom, glomerulus; n.s., not significant; YFP, yellow fluorescent protein.

increased activation of ERK1/2 and Smad1/5 alternative TGF-β signaling pathways. The *Vegfr2* and *Angpt1* genes, which control glomerular endothelial survival and microvascular stability, were downmodulated in glomeruli from diabetic BAMBI$^{-/-}$ mice compared with BAMBI$^{+/+}$ mice. Incubation of glomeruli from nondiabetic BAMBI$^{+/+}$ or BAMBI$^{-/-}$ mice with TGF-β resulted in further downregulation of Angpt1 and Vegfr2 in glomeruli from BAMBI$^{-/-}$ compared with BAMBI$^{+/+}$ mice. The enhanced downregulation of Vegfr2 in glomeruli of diabetic mice by eliminating BAMBI could be localized to glomerular endothelial cells using an H2B-EYFP reporter under the control of Vegfr2/Flk1 regulatory sequences. These results are consistent with a role for BAMBI in modulating the effects of diabetes on glomerular endothelial cells and could thereby alter the permselectivity of the glomerulus. The mechanism involves predominantly modification of alternative TGF-β signaling pathways in the glomerular endothelium. Because BAMBI expression is also downregulated in glomeruli from biopsies of patients with DN, these considerations may also apply to human diabetic glomerulopathy, where therapeutic intervention in alternative signaling pathways of TGF-β may be of therapeutic interest.

BAMBI is considered to function as a nonsignaling pseudo-receptor for the TGF type I receptor family (32). As such, it acts as a dominant negative modulator of kinase signaling pathways activated by members of the TGF family, including TGF-β, bone morphogenic proteins, and activin. Genetic elimination of BAMBI in mice results in only a mild phenotype, characterized by endothelial dysfunction and evidenced by delayed hemostasis, and an activated endothelial phenotype with enhanced in vitro and in vivo angiogenesis (30,31,45). Because diabetic glomerular disease is associated with both TGF-β overexpression and microvascular endothelial alterations, we examined the effect of experimental STZ-induced diabetes on the glomerulus in BAMBI$^{+/+}$ and BAMBI$^{-/-}$ mice. We used STZ-induced diabetes in C57BL/6 mice, a strain that is relatively resistant to the development of diabetic glomerular disease (46,56) and is therefore useful in identifying glomerular changes in response to enhanced TGF-β signaling in the absence of BAMBI. In fact, the very mild degree of albuminuria that occurred at 18 weeks of diabetes in BAMBI$^{+/+}$ mice was significantly increased in BAMBI$^{-/-}$ mice. This occurred without any differences in hyperglycemia, serum creatinine, or blood pressure. As expected, the kidney weight–to–body weight ratio increased after 18 weeks of diabetes in BAMBI$^{+/+}$ and BAMBI$^{-/-}$ mice, consistent with the renal hypertrophy of early diabetes (56).

As further indications of diabetic glomerular disease, we determined mesangial area using semiquantitative, computer-assisted light microscopical evaluation and electron microscopic morphometry of basement membrane thickness and podocyte FP width. Mesangial area and basement membrane thickness increased to a comparable extent in both diabetic BAMBI$^{+/+}$ and BAMBI$^{-/-}$ mice, but FP width increased only in BAMBI$^{-/-}$ mice.

The enhanced podocyte width in diabetic BAMBI$^{-/-}$ mice corresponds to the increased albuminuria observed in these mice. A correlation between podocyte width and proteinuria was noted previously (2,4,10). The reason for the increased proteinuria and podocyte width in the diabetic BAMBI$^{-/-}$ mice is unclear but could be due to altered endothelial and podocyte function and cross-talk with podocytes, as reflected by the changes in Angpt1 and Vegfr2 expression, respectively.

Increased glomerular generation of TGF-β is thought to contribute to diabetic glomerulosclerosis involving canonical TGF-β signaling through Smad2/3 activation and enhanced matrix generation (4). Experimental elimination of Smad3 signaling, however, only reduces mesangial expansion and thickening of the GBM, but, surprisingly, does not reduce albuminuria, in diabetic mouse models (5,6,9,10). Our findings may be of interest in this context because they show the contrasting mirror image in STZ-induced diabetes in BAMBI$^{-/-}$ mice, that is, increased albuminuria, but comparable mesangial and basement membrane expansion with predominantly enhanced Smad1/5 and ERK1/2 activation. We therefore propose that Smad1/5- and ERK1/2-dependent, alternative TGF-β signaling pathways may contribute to the increase in proteinuria in diabetic BAMBI$^{-/-}$ mice.

The observation of alternative TGF-β signaling in glomeruli is reminiscent of that noted for TGF-β signaling in vascular endothelial cells, in which TGF-β signals predominantly through ALK1 alternative pathways rather than through ALK5 receptors and canonical pathways (11,24,26–29). Furthermore, we recently reported that, in endothelial cells, BAMBI interferes predominantly with alternative TGF-β signaling through phosphorylation of ERK1/2 and Smad1/5 (30). The differential effects of BAMBI elimination in diabetic mice in terms of the enhanced activation of ERK1/2 and Smad1/5 also were substantiated by increased mRNA levels for genes classically considered to be regulated by ERK1/2, such as *Raf1*, *Mel2*, and *Ccnd1*, and those regulated by Smad1/5 (48), such as *Atoh8*, *Id3*, and *Snon* (49).

Mitogen-activated protein kinase and ERK1/2 are shown to be activated in glomeruli in diabetic mouse and rat models (12,14,15). In general, ERK1/2 activation has been associated with hypertrophy of glomerular podocytes, mesangial cells, and endothelial cells (15). We therefore hypothesize that elimination of BAMBI in STZ-induced diabetic mice leads to enhanced activation of an alternative TGF-β signaling pathway via ERK1/2 and Smad1/5 activation in diabetes and thereby may contribute to the increased proteinuria in BAMBI$^{-/-}$ mice. This hypothesis would also explain reports that interfering with canonical Smad2/3 signaling in diabetic mice mitigates only glomerular matrix expansion and GBM thickness and not proteinuria (36). The prominent activation of alternative ERK1/2 and Smad1/5 pathways in glomeruli might be due to the high percentage of endothelial cells (30–40%), in which TGF-β signals

predominantly through ALK1 and alternative pathways. While Smad1/5 activation is predominantly dependent on TGF-β, that of ERK1/2 is also influenced by other mitogen-activated protein kinase signaling pathways, which may explain the slightly different effects of BAMBI elimination on their respective activation in glomeruli from diabetic BAMBI$^{+/+}$ versus BAMBI$^{-/-}$ mice (Fig. 4). At present, however, how exactly Smad1/5 and ERK1/2 are activated and in which glomerular cell type, as well as how this contributes to the enhanced ERK1/2 and Smad1/5 activation in glomeruli from diabetic BAMBI$^{-/-}$ mice, remain to be determined.

Endothelial dysfunction is a hallmark of the generalized microvascular disease of diabetes. Changes in the expression of endothelial growth factors and their receptors, such as VEGF-A, angiopoietin 1 and 2, VEGF receptors 1 and 2, and Tie2, were noted in both experimental models and human cases of glomerulosclerosis and proteinuria of diabetes (56–58). Interestingly, we found that glomerular levels of Vegfr2 and Angpt1 mRNA were significantly reduced, especially in diabetic BAMBI$^{-/-}$ mice. To examine whether this might be caused by the observed enhanced TGF-β signaling in BAMBI$^{-/-}$ mice, we incubated glomeruli isolated from BAMBI$^{+/+}$ and BAMBI$^{-/-}$ mice with TGF-β and then analyzed the levels of mRNA for the angiogenic genes. TGF-β inhibited mRNA expression for Vegfr2 and Angpt1 in glomeruli from BAMBI$^{+/+}$ mice—effects that were further enhanced in BAMBI$^{-/-}$ mice. These in vitro results partially mimic the effects of diabetes on glomerular expression of these genes in BAMBI$^{+/+}$ and BAMBI$^{-/-}$ mice and demonstrate that TGF-β inhibits the expression of genes essential for glomerular endothelial function and that a lack of BAMBI accentuates these effects. The effects of TGF-β on the expression of Vegfr2 and Angpt1 might be direct or indirect, but in either case it would eventually affect different glomerular cell types: Vegfr2 is predominantly expressed by glomerular endothelial cells (55), whereas Angpt1 is produced largely by podocytes (58). Dessapt-Baradez et al. (58) showed decreased Angpt1 and Vegfr2 in glomeruli of STZ-induced diabetic mice. Restitution of Angpt1 by inducible podocyte-specific Angpt1 generation resulted in amelioration of proteinuria without reduction of mesangial expansion or the GBM thickness. While the level of mRNA for Vegfr2 was not significantly altered, the amount of phosphorylated Vegfr2 was significantly reduced. Dessapt-Baradez et al. concluded that diabetes induces changes in vascular growth factors and their receptors that result in endothelial dysfunction, contributing to the proteinuria of diabetes. Our results are consistent with this concept.

Finally, to localize the changes in Vegfr2 expression within the glomeruli, we took advantage of a reporter mouse expressing histone yellow fluorescent protein under the control of Vegfr2/Flk regulatory sequences, which has been used to evaluate the expression of Vegfr2 during development (36). In the adult mouse, expression of the reporter is restricted to vascular beds such as the glomerular endothelium, which require persistent expression of VEGF-A by podocytes and VEGF receptor-2 by endothelial cells to maintain normal function and glomerular filtration permselectivity (54,55). Consistent with this concept, we found that in control adult BAMBI$^{+/+}$ mice, glomerular endothelial cells, identified by CD31 staining, coexpressed H2B-EYFP in their nuclei. Induction of diabetes by STZ resulted in decreased intensity of yellow fluorescent protein in glomeruli of BAMBI$^{+/+}$ mice, an effect significantly enhanced in BAMBI$^{-/-}$ mice. These results are in agreement with the mRNA data for Vegfr2 obtained in glomeruli isolated from these mice and further confirm that experimental diabetes causes early endothelial changes, which are accentuated by the elimination of BAMBI.

Overall, our results point to a role for BAMBI in modulating an alternative pathway for TGF-β signaling in the generation of diabetic glomerular changes, in which the glomerular endothelium may play a significant role. BAMBI is downmodulated in isolated glomeruli in both an accelerated model of diabetes in mice with endothelial nitric oxide synthase deficiency and in biopsies from patients with established DN (our data and those reported by Woroniecka et al. [20] and Hodgin et al. [21]). Enhanced activity of an alternative TGF-β pathway in diabetes may be an early step in the development of glomerular endothelial dysfunction, with downregulation of VEGF receptor 2 in endothelial cells and of ANGPT1 in podocytes. This novel mechanism of TGF-β action in the glomerulus may be of significance not only for diabetic proteinuria but also for other diseases leading to glomerulosclerosis.

References

1. Østerby R. Early phases in the development of diabetic glomerulopathy. Acta Med Scand Suppl 1974;574:3–82

2. Dalla Vestra M, Masiero A, Roiter AM, Saller A, Crepaldi G, Fioretto P. Is podocyte injury relevant in diabetic nephropathy? Studies in patients with type 2 diabetes. Diabetes 2003;52:1031–1035

3. Sharma K, Ziyadeh FN. Biochemical events and cytokine interactions linking glucose metabolism to the development of diabetic nephropathy. Semin Nephrol 1997;17:80–92

4.   Ziyadeh FN. Mediators of diabetic renal disease: the case for tgf-Beta as the major mediator. J Am Soc Nephrol 2004;15(Suppl. 1):S55–S57

5.   Sharma K, Jin Y, Guo J, Ziyadeh FN. Neutralization of TGF-beta by anti-TGF-beta antibody attenuates kidney hypertrophy and the enhanced extracellular matrix gene expression in STZ-induced diabetic mice. Diabetes 1996;45:522–530

6.   Ziyadeh FN, Hoffman BB, Han DC, et al. Long-term prevention of renal insufficiency, excess matrix gene expression, and glomerular mesangial matrix expansion by treatment with monoclonal antitransforming growth factor-beta antibody in db/db diabetic mice. Proc Natl Acad Sci U S A 2000;97: 8015–8020

7.   Chen S, Iglesias-de la Cruz MC, Jim B, Hong SW, Isono M, Ziyadeh FN. Reversibility of established diabetic glomerulopathy by anti-TGF-beta antibodies in db/db mice. Biochem Biophys Res Commun 2003;300:16–22

8.   Massagué J. TGF-beta signal transduction. Annu Rev Biochem 1998;67: 753–791

9.   Li J, Qu X, Yao J, et al. Blockade of endothelial-mesenchymal transition by a Smad3 inhibitor delays the early development of streptozotocin-induced diabetic nephropathy. Diabetes 2010;59:2612–2624

10.   Wang A, Ziyadeh FN, Lee EY, et al. Interference with TGF-beta signaling by Smad3-knockout in mice limits diabetic glomerulosclerosis without affecting albuminuria. Am J Physiol Renal Physiol 2007;293:F1657–F1665

11.   Derynck R, Zhang YE. Smad-dependent and Smad-independent pathways in TGF-beta family signalling. Nature 2003;425:577–584

12.   Haneda M, Koya D, Kikkawa R. Cellular mechanisms in the development and progression of diabetic nephropathy: activation of the DAG-PKC-ERK pathway. Am J Kidney Dis 2001;38(4 Suppl 1):S178–S181

13.   Lin CL, Wang FS, Kuo YR, et al. Ras modulation of superoxide activates ERK-dependent fibronectin expression in diabetes-induced renal injuries. Kidney Int 2006;69:1593–1600

14.   Haneda M, Araki S, Togawa M, Sugimoto T, Isono M, Kikkawa R. Mitogen-activated protein kinase cascade is activated in glomeruli of diabetic rats and glomerular mesangial cells cultured under high glucose conditions. Diabetes 1997;46:847–853

15.   Feliers D, Kasinath BS. Erk in kidney diseases. J Signal Transduct 2011; 2011:768512

16.   Sena CM, Pereira AM, Seiça R. Endothelial dysfunction - a major mediator of diabetic vascular disease. Biochim Biophys Acta 2013;1832:2216–2231

17.   Nakagawa T, Kosugi T, Haneda M, Rivard CJ, Long DA. Abnormal angiogenesis in diabetic nephropathy. Diabetes 2009;58:1471–1478

18.   Satchell SC, Tooke JE. What is the mechanism of microalbuminuria in diabetes: a role for the glomerular endothelium? Diabetologia 2008;51:714–725

19.   Ziyadeh FN, Wolf G. Pathogenesis of the podocytopathy and proteinuria in diabetic glomerulopathy. Curr Diabetes Rev 2008;4:39–45

20.   Woroniecka KI, Park AS, Mohtat D, Thomas DB, Pullman JM, Susztak K. Transcriptome analysis of human diabetic kidney disease. Diabetes 2011;60: 2354–2369

21.   Hodgin JB, Nair V, Zhang H, et al. Identification of cross-species shared transcriptional networks of diabetic nephropathy in human and mouse glomeruli. Diabetes 2013;62:299–308

22.   Goumans MJ, Mummery C. Functional analysis of the TGFbeta receptor/Smad pathway through gene ablation in mice. Int J Dev Biol 2000;44:253–265

23.   Pardali E, ten Dijke P. Transforming growth factor-beta signaling and tumor angiogenesis. Front Biosci (Landmark Ed) 2009;14:4848–4861

24.   Seki T, Yun J, Oh SP. Arterial endothelium-specific activin receptor-like kinase 1 expression suggests its role in arterialization and vascular remodeling. Circ Res 2003;93:682–689

25.   Oh SP, Seki T, Goss KA, et al. Activin receptor-like kinase 1 modulates transforming growth factor-beta 1 signaling in the regulation of angiogenesis. Proc Natl Acad Sci U S A 2000;97:2626–2631

26.   Yamashita M, Fatyol K, Jin C, Wang X, Liu Z, Zhang YE. TRAF6 mediates Smad-independent activation of JNK and p38 by TGF-beta. Mol Cell 2008;31: 918–924

27.   Ren B, Deng Y, Mukhopadhyay A, et al. ERK1/2-Akt1 crosstalk regulates arteriogenesis in mice and zebrafish. J Clin Invest 2010;120:1217–1228

28.   Sumpio BE, Yun S, Cordova AC, et al. MAPKs (ERK1/2, p38) and AKT can be phosphorylated by shear stress independently of platelet endothelial cell adhesion molecule-1 (CD31) in vascular endothelial cells. J Biol Chem 2005;280: 11185–11191

29.   Holm TM, Habashi JP, Doyle JJ, et al. Noncanonical TGFβ signaling contributes to aortic aneurysm progression in Marfan syndrome mice. Science 2011; 332:358–361

30.   Guillot N, Kollins D, Gilbert V, et al. BAMBI regulates angiogenesis and endothelial homeostasis through modulation of alternative TGFβ signaling. PLoS One 2012;7:e39406

31.   Guillot N, Kollins D, Badimon JJ, Schlondorff D, Hutter R. Accelerated re-endothelialization, increased neovascularization and erythrocyte extravasation after arterial injury in BAMBI-/- mice. PLoS One 2013;8:e58550

32.   Onichtchouk D, Chen YG, Dosch R, et al. Silencing of TGF-beta signalling by the pseudoreceptor BAMBI. Nature 1999;401:480–485

33.   Seki E, De Minicis S, Osterreicher CH, et al. TLR4 enhances TGF-beta signaling and hepatic fibrosis. Nat Med 2007;13:1324–1332

34.   Yan X, Lin Z, Chen F, et al. Human BAMBI cooperates with Smad7 to inhibit transforming growth factor-beta signaling. J Biol Chem 2009;284:30097–30104

35.   Chen J, Bush JO, Ovitt CE, Lan Y, Jiang R. The TGF-beta pseudoreceptor gene Bambi is dispensable for mouse embryonic development and postnatal survival. Genesis 2007;45:482–486

36.   Fraser ST, Hadjantonakis AK, Sahr KE, et al. Using a histone yellow fluorescent protein fusion for tagging and tracking endothelial cells in ES cells and mice. Genesis 2005;42:162–171

37.   Feng M, Whitesall S, Zhang Y, Beibel M, D'Alecy L, DiPetrillo K. Validation of volume-pressure recording tail-cuff blood pressure measurements. Am J Hypertens 2008;21:1288–1291

38.   Yuen PS, Dunn SR, Miyaji T, Yasuda H, Sharma K, Star RA. A simplified method for HPLC determination of creatinine in mouse serum. Am J Physiol Renal Physiol 2004;286:F1116–F1119

39.   Gu L, Dai Y, Xu J, et al. Deletion of podocyte STAT3 mitigates the entire spectrum of HIV-1-associated nephropathy. AIDS 2013;27:1091–1098

40.   Mallipattu SK, Liu R, Zhong Y, et al. Expression of HIV transgene aggravates kidney injury in diabetic mice. Kidney Int 2013;83:626–634

41.   Chuang PY, Dai Y, Liu R, et al. Alteration of forkhead box O (foxo4) acetylation mediates apoptosis of podocytes in diabetes mellitus. PLoS One 2011;6: e23566

42.   Takemoto M, Asker N, Gerhardt H, et al. A new method for large scale isolation of kidney glomeruli from mice. Am J Pathol 2002;161:799–805

43.   Cohen CD, Frach K, Schlöndorff D, Kretzler M. Quantitative gene expression analysis in renal biopsies: a novel protocol for a high-throughput multicenter application. Kidney Int 2002;61:133–140

44.   Zhao HJ, Wang S, Cheng H, et al. Endothelial nitric oxide synthase deficiency produces accelerated nephropathy in diabetic mice. J Am Soc Nephrol 2006;17:2664–2669

45.   Salles C II, Monkman JH, Ahnstrom J, Lane DA, Crawley JT. Vessel wall bone morphogenetic protein and activin membrane-bound inhibitor (BAMBI) contributes to hemostasis and thrombus stability. Blood 2014;123:2873–2881

46.   Schlöndorff D. Choosing the right mouse model for diabetic nephropathy. Kidney Int 2010;77:749–750

47.   Haneda M, Araki S, Togawa M, Sugimoto T, Isono M, Kikkawa R. Activation of mitogen-activated protein kinase cascade in diabetic glomeruli and mesangial cells cultured under high glucose conditions. Kidney Int Suppl 1997;60:S66–S69

48.   Xie L, Law BK, Chytil AM, Brown KA, Aakre ME, Moses HL. Activation of the Erk pathway is required for TGF-beta1-induced EMT in vitro. Neoplasia 2004;6: 603–610

49.   Morikawa M, Koinuma D, Tsutsumi S, et al. ChIP-seq reveals cell type-specific binding patterns of BMP-specific Smads and a novel binding motif. Nucleic Acids Res 2011;39:8712–8727

50. Simon M, Gröne HJ, Jöhren O, et al. Expression of vascular endothelial growth factor and its receptors in human renal ontogenesis and in adult kidney. Am J Physiol 1995;268:F240–F250

51. Jin J, Sison K, Li C, et al. Soluble FLT1 binds lipid microdomains in podocytes to control cell morphology and glomerular barrier function. Cell 2012; 151:384–399

52. Tufro A, Norwood VF, Carey RM, Gomez RA. Vascular endothelial growth factor induces nephrogenesis and vasculogenesis. J Am Soc Nephrol 1999;10: 2125–2134

53. Satchell SC, Braet F. Glomerular endothelial cell fenestrations: an integral component of the glomerular filtration barrier. Am J Physiol Renal Physiol 2009; 296:F947–F956

54. Eremina V, Jefferson JA, Kowalewska J, et al. VEGF inhibition and renal thrombotic microangiopathy. N Engl J Med 2008;358:1129–1136

55. Sison K, Eremina V, Baelde H, et al. Glomerular structure and function require paracrine, not autocrine, VEGF-VEGFR-2 signaling. J Am Soc Nephrol 2010;21:1691–1701

56. Brosius FC 3rd, Alpers CE. New targets for treatment of diabetic nephropathy: what we have learned from animal models. Curr Opin Nephrol Hypertens 2013;22:17–25

57. Advani A, Gilbert RE. The endothelium in diabetic nephropathy. Semin Nephrol 2012;32:199–207

58. Dessapt-Baradez C, Woolf AS, White KE, et al. Targeted glomerular angiopoietin-1 therapy for early diabetic kidney disease. J Am Soc Nephrol 2014;25:33–42